THE JOURNAL OF BIOLOGICAL CHEMISTRY VOL. 280, NO. 52, pp. 42945–42951, December 30, 2005


# Cathepsin D and $H_2O_2$ Stimulate Degradation of Thioredoxin-1

## *IMPLICATION FOR ENDOTHELIAL CELL APOPTOSIS**

Received for publication, June 27, 2005, and in revised form, October 19, 2005 Published, JBC Papers in Press, November 1, 2005, DOI 10.1074/jbc.M506985200

**Judith Haendeler[‡1], Rüdiger Popp[§], Christine Goy[‡], Verena Tischler[‡], Andreas M. Zeiher[‡], and Stefanie Dimmeler[‡]**

*From the [‡]Molecular Cardiology, Department of Internal Medicine III, and [§]Department of Physiology, University of Frankfurt, Theodor-Stern-Kai 7, 60590 Frankfurt, Germany*

**Cathepsin D (CatD) is a lysosomal aspartic proteinase and plays an important role in the degradation of proteins and in apoptotic processes induced by oxidative stress, cytokines, and aging. All of these stimuli are potent inducers of endothelial cell apoptosis. Therefore, we investigated the role of CatD in endothelial cell apoptosis and determined the underlying mechanisms. Incubation with 100–500 $\mu$M $H_2O_2$ for 12 h induced apoptosis in endothelial cells. To determine a role for CatD, we co-incubated endothelial cells with the CatD inhibitor pepstatin A. Pepstatin A as well as genetic knock down of CatD abolished $H_2O_2$-induced apoptosis. In contrast, overexpression of CatD wild type but not a catalytically inactive mutant of CatD (CatDD295N) induced apoptosis under basal conditions. To gain insights into the underlying mechanisms, we investigated the effect of CatD on reactive oxygen species (ROS) formation. Indeed, knocking down CatD expression reduced $H_2O_2$-induced ROS formation and apoptosis. The major redox regulator in endothelial cells is thioredoxin-1 (Trx), which plays a crucial role in apoptosis inhibition. Thus, we hypothesized that CatD may alter Trx protein levels and thereby promote formation of ROS and apoptosis. Incubation with 100 $\mu$M $H_2O_2$ for 6 h decreased Trx protein levels, whereas Trx mRNA was not altered. $H_2O_2$-induced Trx degradation was inhibited by pepstatin A and genetic knock down of CatD but not by other protease inhibitors. Incubation of unstimulated cell lysates with recombinant CatD significantly reduced Trx protein levels *in vitro*, which was completely blocked by pepstatin A pre-incubation. Overexpression of CatD reduced Trx protein in cells. Moreover, $H_2O_2$ incubation led to a translocation of Trx to the lysosomes prior to the induction of apoptosis. Taken together, CatD induces apoptosis via degradation of Trx protein, which is an essential anti-apoptotic and reactive oxygen species scavenging protein in endothelial cells.**

Lysosomes contain a variety of enzymes for the degradation of proteins, nucleic acids, polysaccharides, and lipids. Among them is the family of the proteolytic enzymes, the cathepsins (1). Cathepsins are subdivided into three classes based on the active site amino acid. Cathepsins are widely distributed in normal tissues (2) and involved in different physiological processes (1). Several studies suggest that cathepsins are involved in the signaling pathways leading to cell death (3, 4). Among the cathepsins, cathepsin D (CatD)[2] seems to have a pivotal role as a cell death mediator (5, 6). Fibroblasts from CatD-deficient mice are more resistant to etoposide and adriamycin-induced apoptosis than fibroblasts from their wild-type littermates (7). Furthermore, microinjection of CatD induces caspase-dependent apoptosis and staurosporine-mediated apoptotic cell death by CatD-triggered cytochrome *c* release (8, 9).

Reactive oxygen species (ROS), such as $H_2O_2$, induce different cellular effects depending on the concentration and cell type. Several studies have documented the involvement of oxidative stress in apoptosis induction. Upon production of high levels of ROS from exogenous or endogenous sources, the redox balance is perturbed, and cells are shifted into a state of oxidative stress (10). These excessively high concentrations of ROS directly cause oxidative damage of DNA, lipids, and proteins and may impair cellular functions, which can result in apoptosis induction in severely damaged cells (11, 12). CatD has been implicated to be involved in oxidative stress-induced apoptotic pathways. Lysosomes, and specifically CatD, have been identified as modulators of oxidative stress-induced apoptosis in alveolar type II cells (6). Moreover, stabilization of lysosomes by imidazoline protected astrocytes from oxidative stress-mediated damage (13).

To protect themselves from oxidative stress, cells possess a set of antioxidative enzymes, which maintain the intracellular reactive oxygen species (ROS) at appropriate levels. Among these antioxidative enzymes are superoxide dismutase and catalase (14). Two other major intracellular redox systems are the thioredoxin and glutathione systems (15, 16). The thioredoxin family includes three proteins, thioredoxin-1 (Trx), thioredoxin-2, and Sp-thioredoxin (17–19). They contain a conserved Cys-Gly-Pro-Cys-active site (cysteine 32 and cysteine 35 within Trx), which is essential for the redox regulatory function of thioredoxins (20). Trx is ubiquitously expressed in mammalian cells, and Trx deficiency leads to a lethal phenotype (20, 21). Recently, we demonstrated that the anti-apoptotic function of physiological concentrations of ROS is dependent on Trx expression in human umbilical venous endothelial cells (HUVEC) (22). Moreover, overexpression of Trx inhibited oxidative stress-induced apoptosis in different cell types, including HUVEC (23–25).

Therefore, we investigated the functional role of CatD on apoptosis in HUVEC and the underlying mechanisms. Our results demonstrate that $H_2O_2$ induced ROS and apoptosis in HUVEC, which was completely blocked by pepstatin A, a CatD inhibitor, as well as by genetic knockdown of CatD. To gain insights into the underlying mechanisms, we investigated the effects of $H_2O_2$ on Trx expression. $H_2O_2$ reduced Trx protein expression prior to the onset of apoptosis. Trx protein was

* This study was supported by the Deutsche Forschungsgemeinschaft (HA2868/3–1) (to J. H.). The costs of publication of this article were defrayed in part by the payment of page charges. This article must therefore be hereby marked "*advertisement*" in accordance with 18 U.S.C. Section 1734 solely to indicate this fact.

[1] To whom correspondence should be addressed: Molecular Cardiology, Dept. of Internal Medicine III, University of Frankfurt, Theodor Stern-Kai 7, 60590 Frankfurt, Germany. Tel.: 49-69-6301-7340; Fax: 49-69-6301-83462; E-mail: j.haendeler@em.uni-frankfurt.de.

[2] The abbreviations used are: CatD, cathepsin D; ROS, reactive oxygen species; Trx, thioredoxin-1; HUVEC, human umbilical venous endothelial cells; HEK, human embryonic kidney; FACS, fluorescence-activated cell sorter.

degraded by CatD *in vitro* and in cells. Thus, Trx degradation may contribute to CatD- and $H_2O_2$-induced apoptosis.

## EXPERIMENTAL PROCEDURES

*Cell Culture*—HUVEC were cultured in endothelial basal medium supplemented with hydrocortisone (1 μg/ml), bovine brain extract (12 μg/ml), gentamicin (50 μg/ml), amphotericin B (50 ng/ml), epidermal growth factor (10 ng/ml), and 10% fetal calf serum (EBM complete). After detachment with trypsin, cells were grown for at least 18 h (26, 27). Human embryonic kidney cells (HEK293) were cultured in Dulbecco's modified Eagle's basal medium with 10% heat-inactivated fetal calf serum.

*Plasmids*—CatD was cloned out of endothelial cell-derived cDNA using the following primers: sense, 5′-GGAATTCGCCATGCAGCCCTCCAGCCTTC-3′ and antisense, 5′-CGAAGCTTGAACAAGAGGCGGGGCAGCCTCG-3′ incorporating EcoRI and HindIII restriction sites. The amplified PCR product was subcloned into pcDNA3.1(−) vector containing a Myc tag (Invitrogen). The catalytically inactive mutant of CatD (CatDD295N) was generated by site-directed mutagenesis (Stratagene) of CatD.

*Transfection*—HUVEC or HEK293 were transfected with CatD plasmid using Superfect (Qiagen) as previously described (25). Phosphorothiolated sense or antisense oligonucleotides (5 μg) corresponding to the CatD sequence (sense, 5′-ATGCAGCCCTCCAGCCTTCTGCC-3′ and antisense, 5′-GGCAGAAGGCTGGAGGGCTGCAT-3′) were transfected into HUVEC using 5 μl of Lipofectamine (Invitrogen). After 5 h, EBM complete was added to the cells, and 2 h later, the cells were incubated with $H_2O_2$ for another 18 h.

*Isolation of RNA and Quantitative Reverse Transcription-PCR*—RNA was isolated using the triazole reagent (Invitrogen). Trx mRNA and GAPDH mRNA were quantified using the Qiagen SYBR Green kit according to the manufacturer's instructions in a light cycler (Roche Applied Science).

*Immunoblot*—After stimulation, HUVEC were scraped off the plates and lysed in radioimmune precipitation assay buffer (50 mM Tris-HCl, pH 8.0, 150 mM NaCl, 1% Nonidet P-40, 0.5% deoxycholic acid, 0.1% sodium dodecyl sulfate). After removing cell debris (15 min, 4 °C, 20,000 × *g*), 60 μg of protein/slot were resolved on SDS-polyacrylamide gels and were blotted onto polyvinylidene difluoride membranes. For detection of protein expression, membranes were incubated with antibodies against Trx, anti-CatD, anti-actin, or anti-tubulin. After incubation for 2 h with the corresponding secondary antibody tagged with horseradish peroxidase, signals were detected by the enhanced chemiluminescence system (Amersham Biosciences).

*Immunostaining*—Cells were fixed with 4% paraformaldehyde for 15 min at room temperature. After permeabilization and blocking (permeabilization solution: 3% bovine serum albumin fraction V, 0.1% Triton X-100, 5% horse serum in phosphate-buffered saline), the cells were incubated with anti-Trx antibody (1:50, BD Biosciences) overnight at 4 °C. After incubation with a fluorescein isothiocyanate-conjugated anti-mouse antibody (1:200, Jackson ImmunoResearch), the cells were incubated with an antibody against CatD (rabbit, 1:50, overnight, 4 °C, Santa Cruz Biotechnology) and with rhodamine red-conjugated Fab fragment anti-rabbit (1:300, 1 h, room temperature, Jackson ImmunoResearch, Inc.). For nuclear staining, cells were incubated with TO-PRO-3 iodide after digestion with RNase A for 15 min (1:4000, 5 min, Molecular Probes). The cells were visualized by confocal microscopy (Zeiss, LSM 510 META; objective, Plan-Apochromat 63×, 1.4 oil).

*Morphological Detection of Cell Death*—Cells were washed with phosphate-buffered saline and fixed in 4% formaldehyde. The cells were stained with 4′,6-diamidino-phenylindole (0.2 μg/ml in 10 mM Tris-HCl, pH 7, 10 mM EDTA, 100 mM NaCl) for 30 min. Thereafter, the cells were washed with phosphate-buffered saline, and nuclear morphology was assessed by fluorescence microscopy. Alternatively, HUVEC were co-transfected with 2.25 μg of plasmid and 0.75 μg of pcDNA3.1 vector encoding for lacZ, and apoptosis was detected by counting the morphological changes of the transfected β-galactosidase-positive cells as described previously (28).

*Detection of Cell Death by FACS*—Detection of cell death was performed by FACS analysis using annexin V-APC binding and 7-amino-actinomycin staining (Pharmingen) as previously described (25). Annexin V is a $Ca^{2+}$-dependent phospholipid-binding protein that has a high affinity to phosphatidylserine, which is exposed on the cell surface of apoptotic cells. In contrast, 7-amino-actinomycin is only cell-permeable when the cell membranes are damaged, indicative of necrotic cell death. Therefore, apoptotic cells are defined as annexin V-positive, 7-amino-actinomycin-negative cells.

*Detection of Intracellular ROS Formation*—Living cells were incubated for dye uptake with 20 μM 2′,7′-dichlorodihydrofluorescein diacetate ($H_2$DCF-DA) for 30 min (Molecular Probes), and ROS formation was measured by analyzing the area under the curve representing the amount of ROS formation in the cells, as previously described (25).

*Measurement of CatD Activity*—CatD activity was measured in HUVEC using a commercially available kit (Oncogene) and detected with an enzyme-linked immunosorbent assay reader at 405 nm.

*In Vitro Degradation of Trx by CatD*—HUVEC were lysed in radioimmune precipitation assay buffer. 100 μg of lysate was incubated with recombinant CatD in 50 mM sodium citrate buffer (pH 3.3) for 30 min at 37 °C. The reaction was stopped using SDS sample dye, and the samples were loaded onto SDS-polyacrylamide gels. After transfer onto polyvinylidene difluoride membranes, human Trx and CatD protein were detected as described above. For specificity of the *in vitro* assay, recombinant CatD was incubated with HUVEC lysates in phosphate-buffered saline (pH 7.2), which did not result in Trx degradation as expected.

*Statistics*—Statistical analysis was performed with Student's *t* test or analysis of variance followed by modified LSD (Bonferroni) test (SPSS Software).

## RESULTS

*Role of CatD in Apoptosis and Endogenous ROS Formation*—To address whether CatD plays a role in endothelial cell apoptosis, HUVEC were incubated with 100 and 200 μM $H_2O_2$ for 6, 12, and 18 h. $H_2O_2$ induced apoptosis in a time-dependent manner, starting at 12 h (Fig. 1*A*). Pre-incubation with the cell-permeable CatD inhibitor pepstatin A (10 μg/ml) inhibited $H_2O_2$- and serum deprivation-mediated apoptosis (Fig. 1*B*). In contrast, incubation with the proteasome complex inhibitor MG132 or with a broad spectrum cysteine inhibitor, E64c, had no protective effect on $H_2O_2$-induced apoptosis (data not shown). Next, we cloned and overexpressed either CatD wild type or a catalytically inactive mutant of CatD (CatDD295N) in HUVEC to determine the effect of CatD on basal apoptosis. As shown in Fig. 1*C*, CatD induced basal apoptosis in HUVEC compared with empty vector, whereas CatDD295N had no effect on apoptosis (Fig. 1*D*), suggesting that CatD activity is required for apoptosis induction and supporting the concept that CatD is indeed involved in the regulation of endothelial cell apoptosis. Next, we examined whether $H_2O_2$ activates CatD. Incubation with $H_2O_2$ led to a 1.7-fold increase in CatD activity in HUVEC as early as 6 h (Fig. 1*E*). Increase in ROS has been discussed as an important prerequisite for cathepsin D/lysosomal-dependent apoptosis induction (29). Furthermore, Yin *et al.* (6) demonstrate that incubation with $H_2O_2$ increases

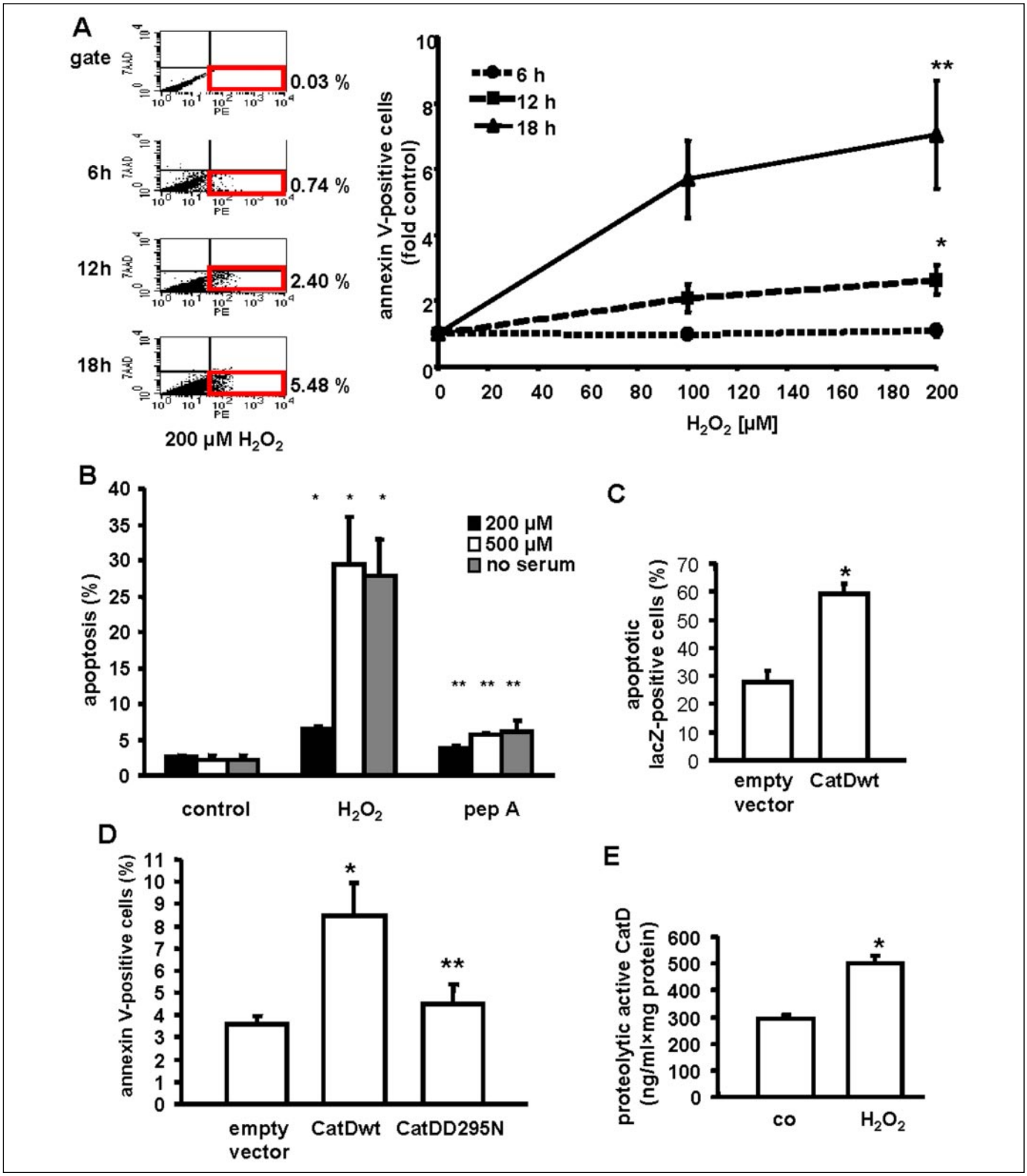


FIGURE 1. *A*, $H_2O_2$-induced apoptosis in a time- and dose-dependent manner. HUVEC were incubated with different $H_2O_2$ concentrations (as indicated) for different times (as indicated). Apoptosis was measured with annexin V/7-amino-actinomycin using FACS analysis. Data are means ± S.D., $n = 3$–5; *, $p < 0.05$ *versus* 6 h + 200 µM $H_2O_2$; **, $p < 0.05$ *versus* 6 h + 200 µM $H_2O_2$. *Left panel*, original FACS blots of 6, 12, and 18 h of 200 µM $H_2O_2$ incubation. *Right panel*, quantitative analysis. *B*, cell-permeable CatD inhibitor pepstatin A (*pep A*) completely abrogated $H_2O_2$- and serum deprivation (*no serum*)-induced apoptosis at 18 h. HUVEC were incubated with $H_2O_2$ (200 and 500 µM) and pepstatin A (10 µg/ml) as indicated. After staining with 4′,6-diamidino-phenylindole, nuclear morphology was assessed by fluorescence microscopy. Data are means ± S.D., $n = 3$; *, $p < 0.05$ *versus* control; **, $p < 0.05$ *versus* $H_2O_2$ or no serum. *C*, overexpression of CatD induced apoptosis in HUVEC. HUVEC were co-transfected with empty vector and lacZ or CatD and lacZ. Apoptosis was detected 24 h later by counting the morphological changes of the transfected β-galactosidase-positive cells as described under "Experimental Procedures." Data are means ± S.D., $n = 6$; *, $p < 0.01$). *D*, overexpression of CatDD295N did not enhance apoptosis. HUVEC were transfected with empty vector, CatD wild type (*CatDwt*), or CatDD295N, and annexin V-positive cells were detected after 24 h by FACS. Data are means ± S.D., $n = 4$; *, $p < 0.05$ *versus* empty vector; **, $p < 0.05$ *versus* CatDwt. *E*, $H_2O_2$ increased CatD activity. HUVEC were incubated with 200 µM $H_2O_2$ for 6 h, and CatD activity was measured. Data are means ± S.D., $n = 8$; *, $p < 0.01$.

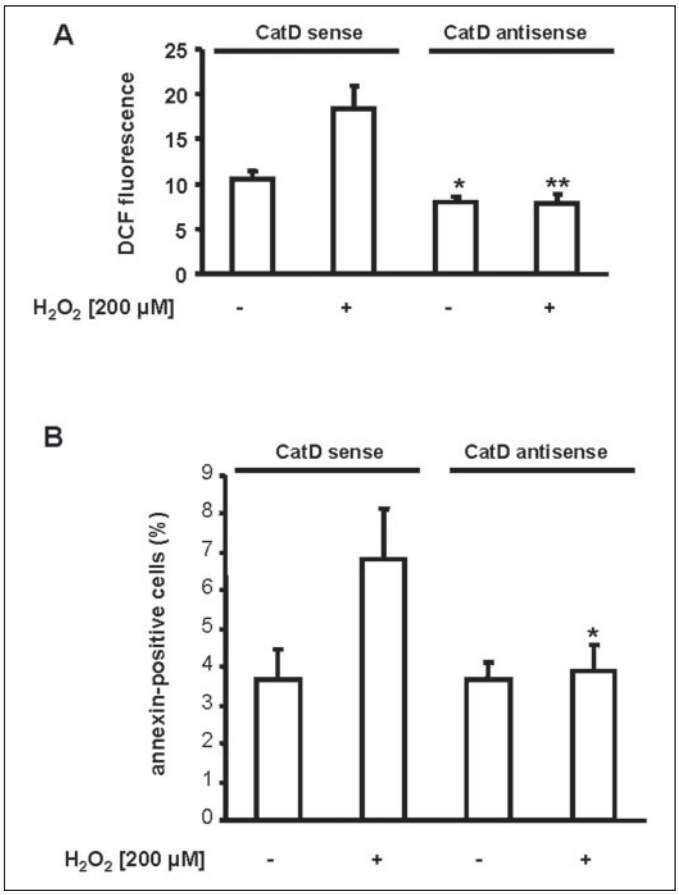


FIGURE 2. **Knocking down CatD expression reduced $H_2O_2$-induced ROS formation and apoptosis.** HUVEC were transfected with sense or antisense oligonucleotides against CatD and incubated with 200 $\mu$M $H_2O_2$ for 18 h. *A*, intracellular ROS was measured using FACS analysis. Data are means ± S.E., $n = 7$; *, $p < 0.01$ *versus* CatD sense; **, $p < 0.05$ *versus* CatD sense + $H_2O_2$. *B*, apoptosis was measured in HUVEC by FACS analysis. Data are means ± S.E., $n = 5$; $p < 0.05$ *versus* CatD sense + $H_2O_2$. *DCF*, dichlorofluorescein.

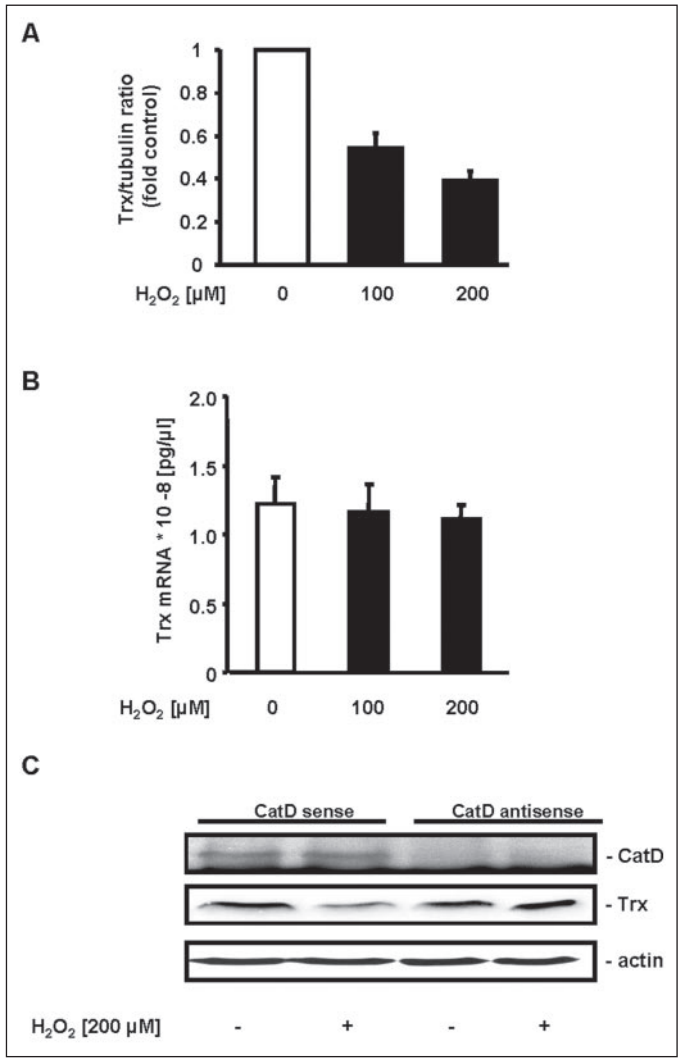


FIGURE 3. *A*, $H_2O_2$ induced Trx degradation in a concentration-dependent manner. HUVEC were incubated with 100 or 200 $\mu$M $H_2O_2$ for 6 h. Immunoblotting with an anti-Trx antibody was performed. Membranes were reprobed with an anti-tubulin antibody. Trx/tubulin ratio was quantified by scanning densitometry using the Scion Image program. Data are means ± S.E., $n = 5$; $p < 0.01$. *B*, $H_2O_2$ did not alter Trx mRNA. HUVEC were incubated with 100 or 200 $\mu$M $H_2O_2$ for 3 h. Quantitative reverse transcription-PCR was performed as described under "Experimental Procedures." Data are means ± S.E., $n = 3$. *C*, HUVEC were transfected with sense or antisense oligonucleotides against CatD and incubated with 200 $\mu$M $H_2O_2$ for 6 h. Immunoblotting with anti-Trx, -CatD, and -actin antibodies was performed. A representative immunoblot is shown.

endogenous ROS formation in astrocytes, resulting in dysfunctional lysosomes and mitochondria and subsequent apoptosis induction. Because CatD overexpression enhanced apoptosis induction, we determined whether CatD plays a role in intracellular ROS formation. Indeed, knocking down CatD expression abrogated $H_2O_2$-induced intracellular ROS formation as measured by FACS analysis (Fig. 2*A*). Moreover, the $H_2O_2$-induced apoptosis was completely abolished in CatD antisense-treated cells (Fig. 2*B*). Thus, knocking down CatD expression inhibited a disturbance of the redox balance and provided protection from $H_2O_2$-induced apoptosis.

*Oxidative Stress-induced Trx Degradation*—One of the most important redox regulators in HUVEC is Trx, which scavenges $H_2O_2$ in cells. Our previous studies demonstrated that overexpression of Trx inhibited $H_2O_2$-induced apoptosis in HUVEC (25). Thus, one may speculate that activation of the protease CatD by $H_2O_2$ leads to a reduction in Trx protein. To test this hypothesis, HUVEC were incubated for 6 h with $H_2O_2$, which resulted in an increase in CatD activity (Fig. 1*E*). Next, we measured Trx protein levels. Indeed, $H_2O_2$ treatment for 6 h decreased Trx protein levels (Fig. 3*A*). To exclude the influence of $H_2O_2$ on Trx mRNA, we performed a quantitative reverse transcription-PCR after incubation with 100 and 200 $\mu$M $H_2O_2$. $H_2O_2$ did not alter TRX mRNA expression (Fig. 3*B*). To test the causal role of CatD in Trx degradation, we next examined whether CatD antisense treatment influenced $H_2O_2$-induced Trx degradation. Indeed, degradation of Trx was completely inhibited in CatD antisense-treated HUVEC (Fig. 3*C*). These results were confirmed by the addition of the cell-permeable CatD inhibitor, pepstatin A. Pepstatin A pre-incubation completely blocked $H_2O_2$-induced degradation of Trx protein (Fig. 4*A*). To exclude that other proteases are involved in Trx degradation, we incubated HUVEC with $H_2O_2$ in the presence of different protease inhibitors. However, using the broad spectrum metalloprotease inhibitor (EDTA, 5 mM), the cysteine protease inhibitor (cell-permeable E64c, 10 $\mu$g/ml), the broad spectrum caspase inhibitor (cell-permeable benzyloxycarbonyl-VAD, 100 $\mu$M), the ubiquitin proteasome inhibitor (MG132, 40 $\mu$M), and the serine protease inhibitor (cell-permeable phenylmethylsulfonyl fluoride (2 mM)) did not inhibit $H_2O_2$-induced Trx degradation (Fig. 4*B*).

To underscore the specific role for CatD in the process of Trx degradation, we incubated unstimulated HUVEC lysates with recombinant CatD in an acidic environment (pH 3.3) and performed immunoblots for Trx protein. Indeed, incubation of unstimulated HUVEC lysates with CatD significantly decreased Trx protein under acidic conditions

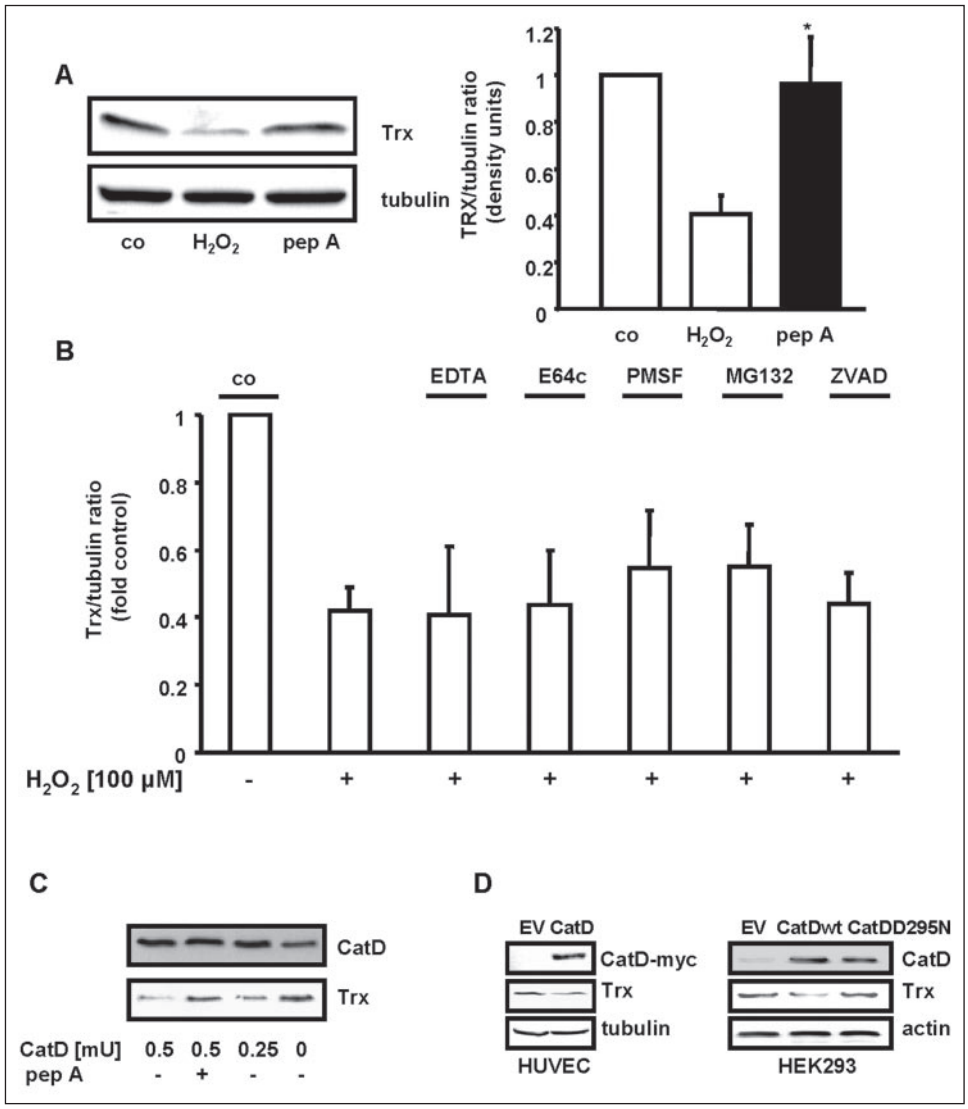


FIGURE 4. *A*, pepstatin A inhibited $H_2O_2$-mediated Trx protein degradation. HUVEC were incubated for 6 h with 100 $\mu$M $H_2O_2$ and pepstatin A (*pep A*) as indicated. Immunoblotting with an anti-Trx antibody was performed. Membranes were reprobed with an anti-tubulin antibody. A representative immunoblot is shown (*left panel*). The Trx/tubulin ratio was quantified by scanning densitometry using the Scion Image program (*right panel*). Data are means ± S.E., $n = 5$; *, $p < 0.05$ *versus* $H_2O_2$. *B*, HUVEC were incubated with $H_2O_2$ and the indicated inhibitors (*EDTA*, *E64c*, phenylmethylsulfonyl fluoride (*PMSF*), *MG132*, and benzyloxycarbonyl-VAD (*ZVAD*)). The Trx/tubulin ratio was quantified by scanning densitometry using the Scion Image program. Data are means ± S.E., $n = 3$–8). *C*, recombinant CatD degrades Trx in unstimulated HUVEC lysates. Unstimulated HUVEC lysates were incubated with recombinant CatD, and immunoblotting with an anti-Trx antibody was performed. Membranes were reprobed with an anti-CatD antibody. Recombinant CatD was pre-incubated with pepstatin A (*pep A*). A representative immunoblot is shown. *D*, overexpression of CatD induced Trx protein degradation. HUVEC and HEK293 were transfected with empty vector (*EV*) or CatD as indicated, and immunoblotting was performed with an anti-Myc or anti-CatD antibody (*upper panels*) and an anti-Trx antibody (*middle panels*). Membranes were reprobed with an anti-tubulin or anti-actin antibody (*lower panels*), respectively.

(Fig. 4*C*; $p < 0.01$). Pre-incubation of recombinant CatD with pepstatin A completely reversed the degradation process (Fig. 4*C*). To further support the role of CatD in Trx protein degradation, we determined Trx protein levels in CatD overexpressing HUVEC. CatD overexpression resulted in a reduction of Trx protein (Fig. 4*D*), To further prove the effect of CatD on Trx protein expression, we used HEK293, which can be transfected with an efficiency of 95%. Indeed, CatD overexpression abrogated Trx protein expression also in HEK293 cells (Fig. 4*D*). Thus, the mechanism in $H_2O_2$- and CatD overexpression-induced apoptosis may require degradation of Trx.

Because CatD is located in the lysosomes and Trx in the cytosol, we next sought to determine where the degradation of Trx takes place. Recent studies (5, 9, 13, 30) suggest that CatD can be released from lysosomes when the lysosomal membrane potential is disturbed and, thereby, translocates to the cytosol and may influence apoptosis pathways. Therefore, we investigated the localization of CatD and Trx after incubation with $H_2O_2$ for 6 h, which is prior to the onset of apoptosis in HUVEC (Fig. 1*A*). After 6 h of $H_2O_2$ incubation, we did not detect a leakage of lysosomal CatD into cytosol (data not shown). In contrast, the cytosolic Trx protein translocated from the cytosol to the lysosomes, suggesting an uptake of Trx into the lysosomes (Fig. 5).

## DISCUSSION

The present study demonstrated that CatD degrades Trx *in vitro* and in cells, which seems to be required for CatD and $H_2O_2$-induced apoptosis in HUVEC. For several years, functions of lysosomal proteases have been described as a nonspecific intracellular degradation machinery acting within the lysosomes. Likewise, lysosomes were suggested to be solely involved in necrotic and autophagic cell death and their role in apoptosis to be limited to the digestion of apoptotic bodies (31). However, the concept has been challenged by several reports. I-cell disease (mucolipidosis type II) fibroblasts, characterized by a general deficiency in lysosomal hydrolases, are partially resistant to apoptosis induced by stress agents, such as staurosporine, sphingosine, and tumor necrosis factor $\alpha$ (32). Likewise, apoptosis induction is reduced in CatD-deficient fibroblasts compared with cells from their wild-type littermates (7, 33). This concept is further supported by our study, demonstrating that overexpression of CatD induced apoptosis, whereas knocking down CatD expression by an antisense approach inhibited $H_2O_2$-mediated apoptosis. An impressive body of evidence now underscores a key role for lysosomes in apoptosis signaling with functional relationships and/or cross-talks with caspases. However, it is not clear what determines the relative contribution of lysosomal enzymes and caspases in

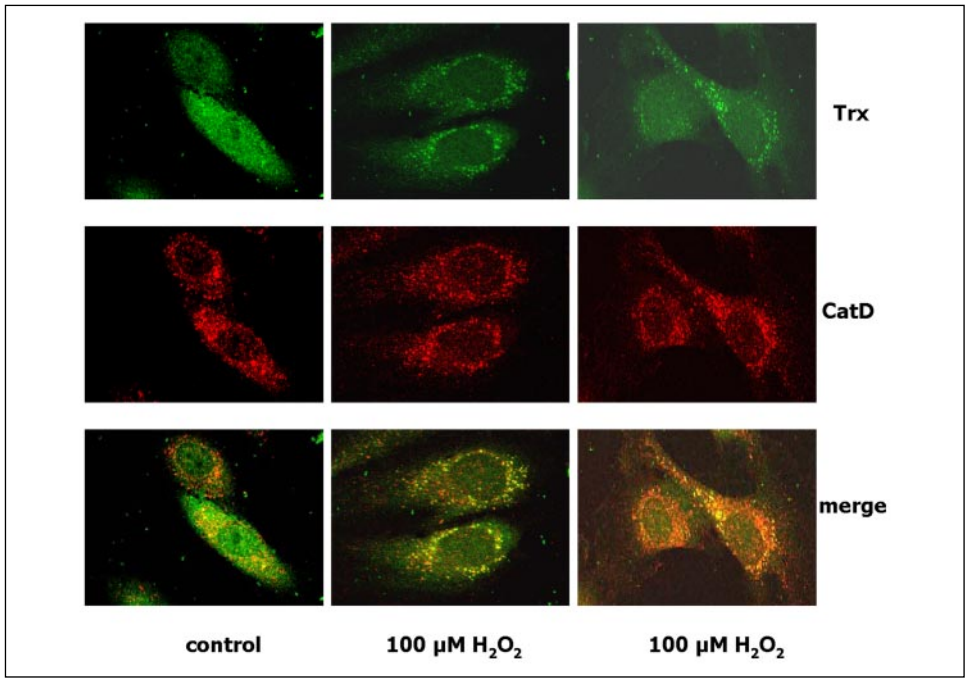


FIGURE 5. **HUVEC were incubated for 6 h with 100 $\mu$M $H_2O_2$, fixed, and immunostained with an antibody against endogenous CatD and endogenous Trx as described under "Experimental Procedures."** *Upper panels* show, in *green*, expression of endogenous Trx and, in *red*, expression of endogenous CatD (*middle panels*). *Lower panels* show the merge of *upper* and *middle panels*.

the initiation and execution of apoptosis. It has been suggested that ROS generation following mitochondrial damage could act as a feedback to the lysosomes, resulting in further activation of lysosomal enzymes and lysosomal breakdown (34, 35), leading to a positive feedback loop and, thereby, to an exacerbation of the caspase cascade. On the other hand short term blockade of intralysosomal digestion by lysosomotropic alkalinizing agents led to an increase in lysosomal pH, consequently a decrease in intralysosomal proteolysis and intracellular ROS formation (36). This is in accordance with the data presented in this study that indicate reduced CatD expression and activity led to a decrease in ROS. Thus, one may speculate that increase in intracellular ROS may alter lysosomal activity prior to mitochondrial damage. Here, we demonstrated that one of the most important intracellular scavengers for $H_2O_2$, Trx, is translocated to the lysosomes and degraded by CatD upon exposure to $H_2O_2$ prior to the onset of apoptosis (Figs. 1*A*, 3*A*, and 5). Moreover, $H_2O_2$-induced Trx degradation occurs prior to the onset of ROS formation (6 h, 200 $\mu$M $H_2O_2$; 102 ± 11% ROS formation compared with the control). These results suggest that Trx degradation results in increased intracellular ROS formation and, thereby, may lead to lysosomal rupture, mitochondrial damage, and apoptosis induction. An important question remains: what is the trigger leading to the translocation of Trx from the cytosol to the lysosomes? Haglund *et al.* (37) demonstrated that a prerequisite for translocation of receptor tyrosine kinases from the plasma membrane to the lysosomes is monoubiquitination of the proteins. The process of monoubiquitination is independent of the ubiquitin-proteasome complex (38), which fits to our study presented here, demonstrating that the specific ubiquitin-proteasome complex inhibitor, MG132, did not block $H_2O_2$-mediated degradation of Trx and apoptosis.

Taken together, our data suggest that translocation of Trx to the lysosomes and degradation of Trx by CatD is a prerequisite for oxidative stress-induced apoptosis induction. Moreover, lysosomal activity and, subsequently, ROS formation seem to precede caspase activation during $H_2O_2$-induced apoptosis in HUVEC.

*Acknowledgment—We thank Carmen Schön for expert technical assistance.*

## REFERENCES


1. Barrett, A. J. (2004) *Curr. Opin Drug. Discovery Dev.* **7,** 334–341
2. Reid, W. A., Valler, M. J., and Kay, J. (1986) *J. Clin. Pathol.* (*Lond.*) **39,** 1323–1330
3. Leist, M., and Jaattela, M. (2001) *Cell Death Differ.* **8,** 324–326
4. Salvesen, G. S. (2001) *J. Clin. Investig.* **107,** 21–22
5. Jaattela, M., Cande, C., and Kroemer, G. (2004) *Cell Death Differ.* **11,** 135–136
6. Yin, L., Stearns, R., and Gonzalez-Flecha, B. (2005) *J. Cell. Biochem.* **94,** 433–445
7. Wu, G. S., Saftig, P., Peters, C., and El-Deiry, W. S. (1998) *Oncogene* **16,** 2177–2183
8. Roberg, K., Kagedal, K., and Ollinger, K. (2002) *Am. J. Pathol.* **161,** 89–96
9. Johansson, A. C., Steen, H., Ollinger, K., and Roberg, K. (2003) *Cell Death Differ.* **10,** 1253–1259
10. Parman, T., Wiley, M. J., and Wells, P. G. (1999) *Nat. Med.* **5,** 582–585
11. Inoue, M., Sato, E. F., Nishikawa, M., Hiramoto, K., Kashiwagi, A., and Utsumi, K. (2004) *Redox. Rep.* **9,** 237–247
12. Andersen, J. K. (2004) *Nat. Med.* **10,** S18–S25
13. Choi, S. H., Choi, D. H., Lee, J. J., Park, M. S., and Chun, B. G. (2002) *Free Radic. Biol. Med.* **32,** 394–405
14. Fujii, J., and Taniguchi, N. (1999) *Free Radic. Res.* **31,** 301–308
15. Holmgren, A. (2000) *Antioxid Redox Signal* **2,** 811–820
16. Nordberg, J., and Arner, E. S. (2001) *Free Radic. Biol. Med.* **31,** 1287–1312
17. Taniguchi, Y., Taniguchi-Ueda, Y., Mori, K., and Yodoi, J. (1996) *Nucleic Acids Res.* **24,** 2746–2752
18. Spyrou, G., Enmark, E., Miranda-Vizuete, A., and Gustafsson, J. (1997) *J. Biol. Chem.* **272,** 2936–2941
19. Miranda-Vizuete, A., Ljung, J., Damdimopoulos, A. E., Gustafsson, J. A., Oko, R., Pelto-Huikko, M., and Spyrou, G. (2001) *J. Biol. Chem.* **276,** 31567–31574
20. Holmgren, A. (1989) *J. Biol. Chem.* **264,** 13963–13966
21. Matsui, M., Oshima, M., Oshima, H., Takaku, K., Maruyama, T., Yodoi, J., and Taketo, M. M. (1996) *Dev. Biol.* **178,** 179–185
22. Haendeler, J., Tischler, V., Hoffmann, J., Zeiher, A. M., and Dimmeler, S. (2004) *FEBS Lett.* **577,** 427–433
23. Andoh, T., Chock, P. B., and Chiueh, C. C. (2002) *J. Biol. Chem.* **277,** 9655–9660
24. Shioji, K., Kishimoto, C., Nakamura, H., Masutani, H., Yuan, Z., Oka, S., and Yodoi, J. (2002) *Circulation* **106,** 1403–1409
25. Haendeler, J., Hoffmann, J., Tischler, V., Berk, B. C., Zeiher, A. M., and Dimmeler, S. (2002) *Nat. Cell Biol.* **4,** 743–749
26. Haendeler, J., Weiland, U., Zeiher, A. M., and Dimmeler, S. (1997) *Nitric Oxide* **1,** 282–293
27. Dimmeler, S., Haendeler, J., Rippmann, V., Nehls, M., and Zeiher, A. M. (1996) *FEBS Lett.* **399,** 71–74
28. Dimmeler, S., Haendeler, J., Galle, J., and Zeiher, A. M. (1997) *Circulation* **95,** 1760–1763
29. Raymond, M. A., Mollica, L., Vigneault, N., Desormeaux, A., Chan, J. S., Filep, J. G., and Hebert, M. J. (2003) *FASEB J.* **17,** 515–517
30. Kagedal, K., Johansson, U., and Ollinger, K. (2001) *FASEB J.* **15,** 1592–1594

31. Leist, M., and Jaattela, M. (2001) *Nat. Rev. Mol. Cell Biol.* **2,** 589–598
32. Tardy, C., Tyynela, J., Hasilik, A., Levade, T., and Andrieu-Abadie, N. (2003) *Cell Death Differ.* **10,** 1090–1100
33. Neuzil, J., Zhao, M., Ostermann, G., Sticha, M., Gellert, N., Weber, C., Eaton, J. W., and Brunk, U. T. (2002) *Biochem. J.* **362,** 709–715
34. Zhao, M., Antunes, F., Eaton, J. W., and Brunk, U. T. (2003) *Eur. J. Biochem.* **270,** 3778–3786
35. Cirman, T., Oresic, K., Mazovec, G. D., Turk, V., Reed, J. C., Myers, R. M., Salvesen, G. S., and Turk, B. (2004) *J. Biol. Chem.* **279,** 3578–3587
36. Yu, Z., Persson, H. L., Eaton, J. W., and Brunk, U. T. (2003) *Free Radic. Biol. Med.* **34,** 1243–1252
37. Haglund, K., Sigismund, S., Polo, S., Szymkiewicz, I., Di Fiore, P. P., and Dikic, I. (2003) *Nat. Cell Biol.* **5,** 461–466
38. Hicke, L. (2001) *Nat. Rev. Mol. Cell Biol.* **2,** 195–201